BR8714919

8. Title INPE-3868-PRE/926

ELECTRON BERNSTEIN WAVE CURRENT DRIVE IN THE START-UP PHASE OF A TOKAMAK DISCHARGE

9. Authorship A. Montes
G.O. Ludwig

Antonio Montes
Responsible author

INSTITUTO DE PESQUISAS ESPACIAIS

1. Publication Nº	2. Version	3. Date	5. Distribution
INPE-3868-PRE/926		*April, 1986*	☐ Internal ☒ External ☐ Restricted

4. Origin: *DMS* Program: *PLASMA*

6. Key words - selected by the author(s)
NON-INDUCTIVE CURRENT DRIVE
ELECTRON BERNSTEIN
TOKAMAK DISCHARGE
START-UP PHASE

7. U.D.C.: *533.9*

8. Title: *INPE-3868-PRE/926*

ELECTRON BERNSTEIN WAVE CURRENT DRIVE IN THE START-UP PHASE OF A TOKAMAK DISCHARGE

10. Nº of pages: *18*

11. Last page: *12*

12. Revised by

Abraham C.-L. Chian

9. Authorship *A. Montes*
G.O. Ludwig

Responsible author

13. Authorized by

Marco Antonio Raupp
Director General

14. Abstract/Notes

Current drive by electron Bernstein waves in the start-up phase of tokamak discharges is studied. A general analytical expression is derived for the figure of merit J/P_d associated with these waves. This is coupled with a ray tracing code, allowing the calculation of the total current generated per unit incident power in realistic tokamak conditions. The results show that electron Bernstein waves can drive substantial currents even at very low electron temperatures.

15. Remarks *This paper will be submitted to Plasma Physics.*

ELECTRON BERNSTEIN WAVE CURRENT DRIVE IN THE START-UP PHASE OF A TOKAMAK DISCHARGE

A. MONTES and G.O. LUDWIG

Instituto de Pesquisas Espaciais - INPE

C.P. 515 - 12200 São José dos Campos, SP, Brasil

ABSTRACT

Current drive by electron Bernstein waves in the start-up phase of tokamak discharges is studied. A general analytical expression is derived for the figure of merit J/P_d associated with these waves. This is coupled with a ray tracing code, allowing the calculation of the total current generated per unit incident power in realistic tokamak conditions. The results show that electron Bernstein waves can drive substantial currents even at very low electron temperatures.

1. INTRODUCTION

The use of electron cyclotron radiation to assist the start-up phase of tokamak discharges is of great interest due to the possibility of preionizing and heating the discharge through the radiation barrier to ~100eV. This would result in a considerable reduction of the loop voltage during the initial stage of the main discharge, with a consequent saving of the ohmic transformer flux.

Preionization with the aid of electron cyclotron radiation has been demonstrated to be an effective means of reducing the voltage required for break-down in tokamaks (Lashmore-Davies, 1981; Gilgenbach et al., 1981). On the other hand, the electron temperature attained during these experiments was always much smaller than the desired 100eV. This is in marked contrast to stellarators (Iiyoshi et al., 1982) where temperatures as high as 1.1keV have been achieved. As pointed out by Lashmore-Davies (1981), the difference is evidently due to the existence of a plasma-magnetic field equilibrium in the stellarator. He suggests that the confinement of the preionized plasma may be improved by utilizing part of the electron cyclotron radiation to drive a toroidal current and hence to create the required equilibrium configuration.

The generation of toroidal current by electromagnetic waves in the electron cyclotron frequencies range, due to the Fisch-Boozer mechanism (Fisch and Boozer, 1980), has been shown theoretically (Cordey et al., 1982; Karney and Fisch, 1985) to be an effective scheme for noninductive current drive during the main discharge phase. These calculations rely on the absorption of extraordinary (X) or ordinary (O) waves at the electron cyclotron resonance. It is therefore not

surprising that during the start-up phase very little current generation by these modes is expected, keeping in mind that practically none of the incident wave energy is absorbed at the electron cyclotron resonance. However, this reasoning neglects the longitudinal electron Bernstein wave (EBW). Current drive, during the main discharge, by EBW at the second cyclotron harmonic has been investigated in slab geometry (Hsu et al., 1983; Owen et al., 1984), and it was found that the local figure of merit J/P_d due to EBW can be much larger than that obtained for the X or O-mode. In this paper, it is shown that EBW, at the fundamental electron cyclotron frequency, is very effective in generating current even in the conditions prevailing during the start-up phase.

It is well known (Airoldi Crescentini and Orefice, 1980; Pesic, 1984) that extraordinary waves launched from the high magnetic field side can be mode converted into electron Bernstein waves, near the upper hybrid resonance surface (defined by $\omega^2 = \omega_{pe}^2(r) + \Omega_e^2(r)$, where ω is the incident wave frequency, ω_{pe} and Ω_e are the local electron plasma and electron cyclotron frequencies, respectively). Upon conversion, EBW with finite $k_{\parallel}$ travel back toward the electron cyclotron resonance surface, where $\omega = \Omega_e(x)$, near which the group velocity of the wave tends to become aligned with the magnetic field (Airoldi Crescentini and Orefice, 1980) and the wave undergoes strong electron cyclotron collsionless damping (Pesic, 1984), transferring all its energy to the plasma electrons.

The physical mechanism reponsible for the generation of current by EBW is the same as for the generation of current by X or O-mode, namely the EBW selectively heats electrons moving in one direction

along the magnetic field lines, creating an asymmetric resistivity in the plasma, and thus producing an imbalance in the velocity distribution function in the parallel direction which then gives rise to a current.

2. DERIVATION OF THE FIGURE OF MERIT J/P_d

The current generated by the EBW can be estimated by means of a Fokker-Planck treatment. In this approach, the time evolution of the electron velocity distribution function, due to the interaction of the plasma electrons and the EBW, can be represented as

$$\frac{\partial f_e}{\partial t} = \left[\frac{\partial f_e}{\partial t}\right]_{coll} + \left[\frac{\partial f_e}{\partial t}\right]_{w} \tag{1}$$

where $(\partial f_e/\partial t)_{coll}$ is the Coulomb collision term and $(\partial f_e/\partial t)_w$ represents the velocity space diffusion due to the presence of the oscillating wave field. For the purpose of the present calculation, electron-electron collisions are neglected (they will be included in the numerical calculations in an ad hoc manner) so that the Coulomb collision term includes only electron-ion collisions and is given by

$$\left[\frac{\partial f_e}{\partial t}\right]_{coll} = \frac{D_c(v)}{v^2 \sin\Theta} \frac{\partial}{\partial \Theta}\left[\sin\Theta \frac{\partial f_e}{\partial t}\right]. \tag{2}$$

Here $D_c(v)=n_i\Gamma_{ei}/2v$, $\Gamma_{ei}=(Ze^2)^2 \ln\Lambda_{ei}/4\pi\varepsilon_0^2 m_e^2$, $\tan\Theta \equiv v_\perp/v_\parallel$, Z is the effective plasma ionic charge, m_e and v are the electron mass and velocity respectively, $n_i = n_e$ is the electron number density, and $\ln\Lambda_{ei}$ is the Coulomb logarithm.

The velocity space diffusion caused by electron Bernstein waves was derived by Kennel and Engelmann (1966) and, for $k_\parallel \ll k_\perp$, reduces to

$$\left(\frac{\partial f_e}{\partial t}\right)_W = \frac{1}{v_\perp}\frac{\partial}{\partial v_\perp}\left[v_\perp D(v_\perp, v_\parallel)\frac{\partial f_e}{\partial v_\perp}\right], \tag{3}$$

where

$$D(v_\perp, v_\parallel) = \frac{2\pi}{\varepsilon_0}\left(\frac{e}{m_e}\right)^2 \sum_{\vec{k}} U_{\vec{k}} \sum_n \left(\frac{n\Omega_e}{kv_\perp}\right)^2 J_n^2\left(\frac{k_\perp v_\perp}{\Omega_e}\right)\delta(\omega - k_\parallel v_\parallel - n\Omega_e). \tag{4}$$

Here J_n is the Bessel function of order n, $U_{\vec{k}} = \varepsilon_0 |E_{\vec{k}}|^2/2$ is the electrostatic energy density, and $\vec{k}$ is the wavevector. In deriving eq. (3) from the general expression given in Kennel and Engelmann (1966) one finds that in the present situation the diffusion occurs mainly in the perpendicular direction. Only the fundamental (n=1) contribution will be kept in the following calculations.

For sufficiently small wave amplitude, the velocity distribution function can be approximated by

$$f_e = F_M + f_e', \tag{5}$$

where F_M is a Maxwellian and f_e' is a small perturbation.

In steady-state, $\partial f_e/\partial t = 0$ and the linearized Fokker-Planck equation becomes an equation for the perturbation f_e':

$$\frac{D_c(v)}{v^2}\frac{\partial}{\partial \mu}\left[(1-\mu^2)\frac{\partial f_e'}{\partial \mu}\right] + \frac{1}{v_\perp}\frac{\partial}{\partial v_\perp}\left[v_\perp D(v_\perp, v_\parallel)\frac{\partial F_M}{\partial v_\perp}\right] = 0, \tag{6}$$

where $\mu=\cos\theta$. Expanding f_e' in a series of Legendre polynomials

$$f_e' = F_M \sum_{l=1}^{\infty} a_l(v) P_l(\mu), \tag{7}$$

substituting it into eq. (6) and using the orthogonality relation for the Legendre polynomials, one can obtain expressions for the coefficients $a_l(v)$.

The electron current density is given by

$$J = -e \int v_\parallel f_e d^3v,$$

$$= -2\pi e \int_0^\infty v^3 dv \int_{-1}^{1} \mu f_e' \, d\mu. \tag{8}$$

Therefore, only the term $l=1$ in the expansion gives a nonzero contribution to the current. After some algebra, one finds

$$J = -\frac{6\sqrt{\pi}\, Ze^3 v_e}{m_e^2 \Gamma_{ei}} \sum_{\vec{k}} \frac{k_\perp^2}{|k_\parallel| k^2} \left| \frac{E_{\vec{k}}}{2} \right|^2 u_0 e^{-u_0^2} I(u_0, k_\perp^2 r_e^2), \tag{9}$$

where

$$u_0 = \frac{\omega - \Omega_e}{k_\parallel v_e}, \tag{10}$$

$$I(u_0, k_\perp^2 r_e^2) = \frac{4}{k_\perp^2 r_e^2} \int_0^\infty dx \, (x + u_0^2)^{1/2} \, e^{-x} \, J_1^2 \, (k_\perp r_e \sqrt{x}), \tag{11}$$

$v_e = \sqrt{2k_B T_e / m_e}$ is the electron thermal velocity and $r_e = v_e/\Omega_e$ is the electron Larmor radius.

The deposited power density is given by

$$P_d = \int \frac{1}{2} m_e v^2 \left(\frac{\partial f_e}{\partial t}\right)_W v_\perp dv_\perp dv_\parallel . \qquad (12)$$

Substituting eq. (3) into (12), integrating and using expression (9) for the current density, one finally obtains the EBW current generation efficiency

$$\frac{J}{P_d} = - \frac{24\pi\epsilon_0^2}{e^3} \frac{k_B T_e}{Z n_e \ln\Lambda_{ei}} \frac{u_0 I(u_0, k_\perp^2 r_e^2)}{(4/k_\perp^2 r_e^2)\exp(-k_\perp^2 r_e^2/2) I_1(k_\perp^2 r_e^2/2)} \qquad (13)$$

in A.m/W. Here I_1 is the modified Bessel function of order 1.

3. NUMERICAL CALCULATIONS

The above xpression for the current efficiency has been incorporated into a ray tracing code (Fielding, 1980), allowing the calculation of the current profile in realistic tokamak conditions. The ray tracing code provided values of u_0, $k_\perp r_e$, T_e and n_e at each point along the rays, which were then used to calculate the current density at those points. The code calculates the contribution of each ray to the current between r and r + dr, which are added up for all rays to give the final current density profile. This is integrated in the radial direction to give the total current per unit injected power.

The plasma equilibrium is modelled by parabolic radial profiles for the electron density and temperature.

$$n_e(r) = n_e(0) \left(1 - \frac{r^2}{a^2}\right). \qquad (14)$$

$$T_e(r) = T_e(0)\left[1 - \frac{r^2}{a^2}\right], \tag{15}$$

and the toroidal magnetic field is given by

$$B_T(\vec{r}) = B_T(0) \Big/ \left[1 + \frac{x}{R_0}\right], \tag{16}$$

where $r^2 = x^2 + y^2$, a and R_0 are the minor and major radius, respectively. The rays are launched from the high magnetic field side with a conical distribution of initial wave vectors to represent a typical antenna pattern.

The parameters used in the calculations have been chosen to simulate the preionization stage of the COMPASS tokamak (COMPASS PROJECT, 1984). They are $R_0 = 0.55$m, $a = 0.22$m, $n_e(0) = 2 \times 10^{18}$m^{-3}, $T_e(0) = 50$eV and $B_T(0) = 1.07$T. The frequency of the incident radiation is 28GHz, polarized in the X-mode. The launching position is $x_0 = -a/\sqrt{2}$, $y_0 = a/\sqrt{2}$, the full cone angular aperture is 20^0, and the cone axis makes an angle of 120^0 with the axial magnetic field. The poloidal and equatorial projections of the ray trajectories for this case are shown in Figs. 1 and 2, respectively. Fig. 3 displays the absorption per unit parallel velocity interval as a function of the normalized resonant parallel velocity u_0. It shows a small absorption of the X-mode around the electron cyclotron resonance ($u_0 = 0$) and a much larger absorption peak associated with the EBW. The current density radial profile is shown in Fig. 4. Electron--electron collisions have been included approximately in these calculations by dividing the values of J/P_d obtained from eq. (13)

by $(5+Z)$. This approximation has been derived in Fisch and Boozer (1980) and shown (Cordey et al., 1982) to be very good for $u_0 \geq 3$. In the present calculations we have used $Z = 1$. For this condition, the calculated overall efficiency is $I/P = 0.11$ A/W, indicating that this mechanism is able to generate a substantial plasma current in the start-up phase.

The generation of current by the EBW will cause an enhancement of the plasma confinement, with a consequent increase in the electron temperature. As the temperature increases, a larger fraction of the power in the X-mode will be damped on the high field side of the electron cyclotron resonance. This will produce a current flowing in the opposite direction to that generated by the EBW. Therefore, as the electron temperature increases, the overall current reaches a maximum and then starts to decrease, changing sign for sufficiently large temperatures. This behaviour is shown in Fig. 5. In addition, the temporal variation of the current will also depend upon the temporal variation of the electron density and poloidal magnetic field. In the case of the poloidal magnetic field, it is important to choose the appropriate launching position in order to avoid a change of sign in $k_{\parallel}$, due to the rotational transform associated with increasing B_p. This dependence upon quantities whose values are changing in time in an unknown fashion makes it very difficult to predict theoretically what is the optimum condition for the generation of current by EBW. It is clear that at some point in time the RF source will have to be switched off to avoid current reversal, and thereafter other current drive scheme will

have to be used. This can be any of a variety of methods available, including electron cyclotron resonance absorption in the appropriate conditions. Nonetheless, the results in Fig. 5 indicate that with an appropriate choice of launching conditions, current generation by EBW remains efficient long enough to allow the discharge to burn through the radiation barrier.

4. CONCLUSIONS

We have found that electron Bernstein waves can drive plasma current with considerable efficiency even at low electron temperatures. This makes them an ideal candidate for current drive in the start-up phase of tokamak discharges. Microwave preionization in the vicinity of the electron cyclotron resonance has been demonstrated to be an effective means of reducing the voltage required for breakdown in tokamaks. The possibility of simultaneously generating a current at this stage of the discharge might lead to an enhanced plasma confinement, allowing the discharge to burn through the radiation barrier. This would result in a substantial reduction in the volt.second consumption and consequently in the cost of the poloidal field system.

The lack of theory for the temporal evolution of the electron density and temperature and the poloidal magnetic field makes it difficult to predict the best launch conditions. Nevertheless, the present results give the experimental optimization of the process some guidelines, indicating that the angle of incidence should be chosen to avoid a change of sign of $k_{\parallel}$ as the poloidal magnetic field varies.

ACKNOWLEDGEMENTS

One of the authors (A.M.) would like to thank C.N. Lashmore-Davies for many suggestions and helpful comments. Thanks are also due to M.O'Brien, B. Lloyd, A.C. Riviere and D.F.H. Start for many stimulating discussions, and to W.M. Lomer and the Culham Laboratory for the hospitality extended to him during part of this work. The same author received financial support from the Conselho Nacional de Desenvolvimento Científico e Tecnológico - CNPq (Brazil).

REFERENCES

AIROLDI CRESCENTINI, A., OREFICE, A. (1980) J. Plasma Physics 23 (2), 209.

COMPASS PROJECT (1984), Culham Laboratory Report CR83.240 (rev. 2/84).

CORDEY, J.G., EDLINGTON, T., START, D.F.H. (1982) Plasma Physics 24 (1), 73.

FIELDING, P., (1980) Private Communication.

FISCH, N.J., BOOZER, A.H. (1980) Phys. Rev. Lett. 45 (9), 720.

GILGENBACH, R.M., READ, M.E., HACKETT, K.E., LUCEY, R.F., GRANATSTEIN, V.L., ENGLAND, A.C., LORING, C.M., WILGEN, J.B., ISLER, R.C., PENG. Y.-K.M., BURRELL, K.H., ELDRIDGE, O.C., HACKER, M.P., KING, P.W., KULCHAR, A.G., MURAKAMI, M., RICHARDS, R.K. (1981), Nuclear Fusion 21 (3), 319.

HSU, J.Y., CHAN, V.S., MCCLAIN, F.W. (1983) Phys. Fluids 26 (11), 3300; OWEN, J.A., CAIRNS, R.A., LASHMORE-DAVIES, C.N. (1984) Proceedings of the 4th Int. Symposium on Heating in Toroidal Plasmas (Rome, Italy), Vol. II, 882.

IIYOSHI, A., SATO, M., MOTOJIMA, O., MUTOH, T., SUDO, S., IIMA, M. KINOSHITA, S., KANEKO, H., ZUSHI, H.; BESSHOU, S., KONDO, K., MIZUUCHI, T., MORIMOTO, S., UO, K. (1982) Phys. Rev. Lett. 48 (11)720.

KARNEY, C.F.F., FISCH, N.J. (1985) Phys. Fluids 28 (1), 116.

KENNEL, C.F., ENGELMANN, F. (1966) Phys. Fluids 9 (12), 2277.

LASHMORE-DAVIES, C.N. (1981), INTOR-European Contributions to the 3rd Workshop, EUR FU BRU/XII - 2/81/ED V70

PESIC, S. (1984) Physica 125C, 118.

FIGURE CAPTIONS

Fig. 1 - Minor cross section projection of ray trajectories. The plasma parameters values are displayed. Each cross on a ray marks a 5% decrease in the power carried by the ray. The vertical dashed line marks the position $\omega = \Omega_e(y)$.

Fig. 2 - Major cross section projection of ray trajectories.

Fig. 3 - Power deposited per unit parallel velocity interval.

Fig. 4 - Current density profile. The total current is the integral of J(r) over the minor cross section. P is the total incident power.

Fig. 5 - Variation of the figure of merit (I/P) with the central electron temperature ($T_e(0)$). Different curves show results for different angles of incidence. The angles are measured away from the normal to the magnetic field.

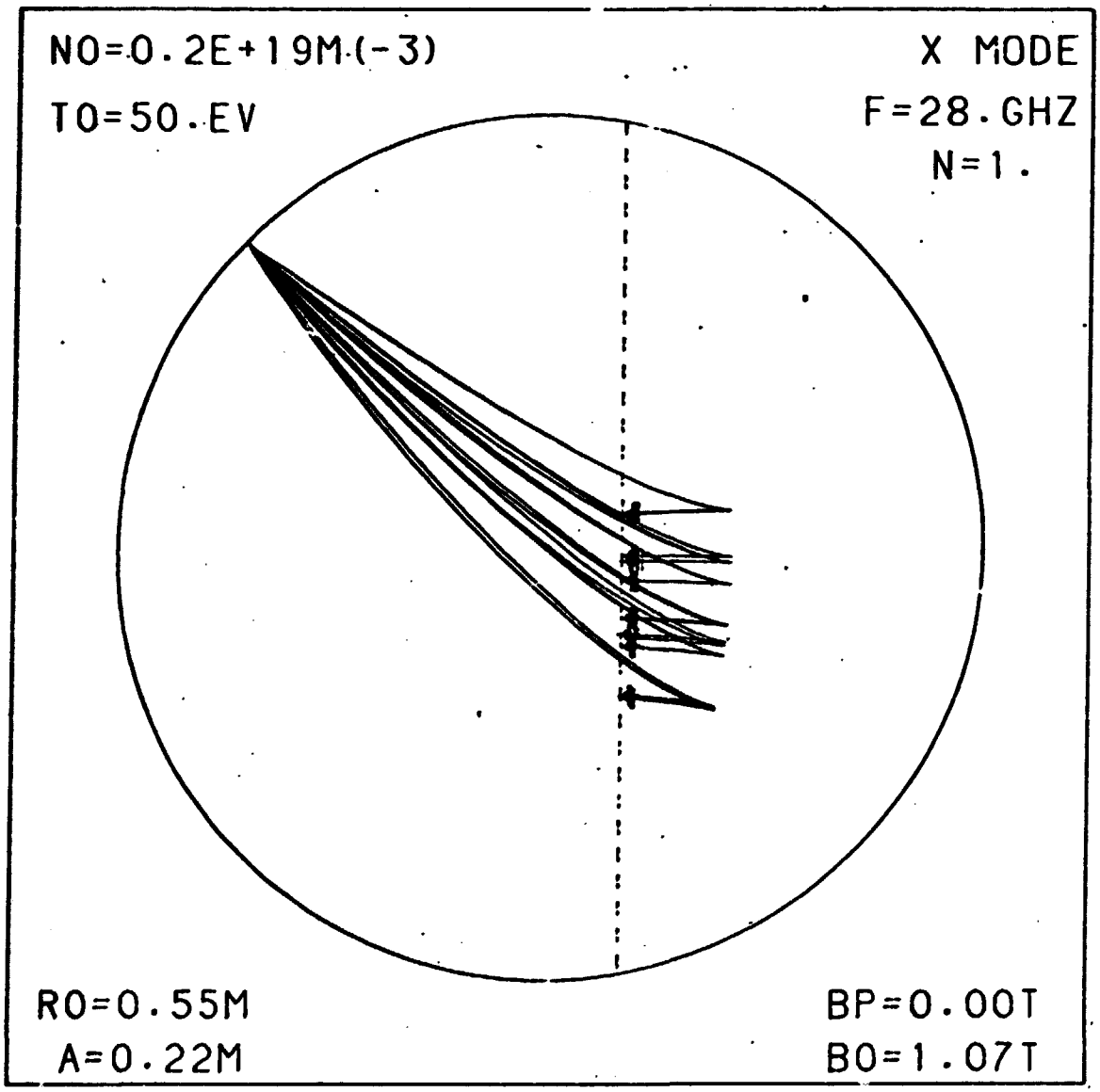

Fig. 1 - A. Montes and G.O. Ludwig

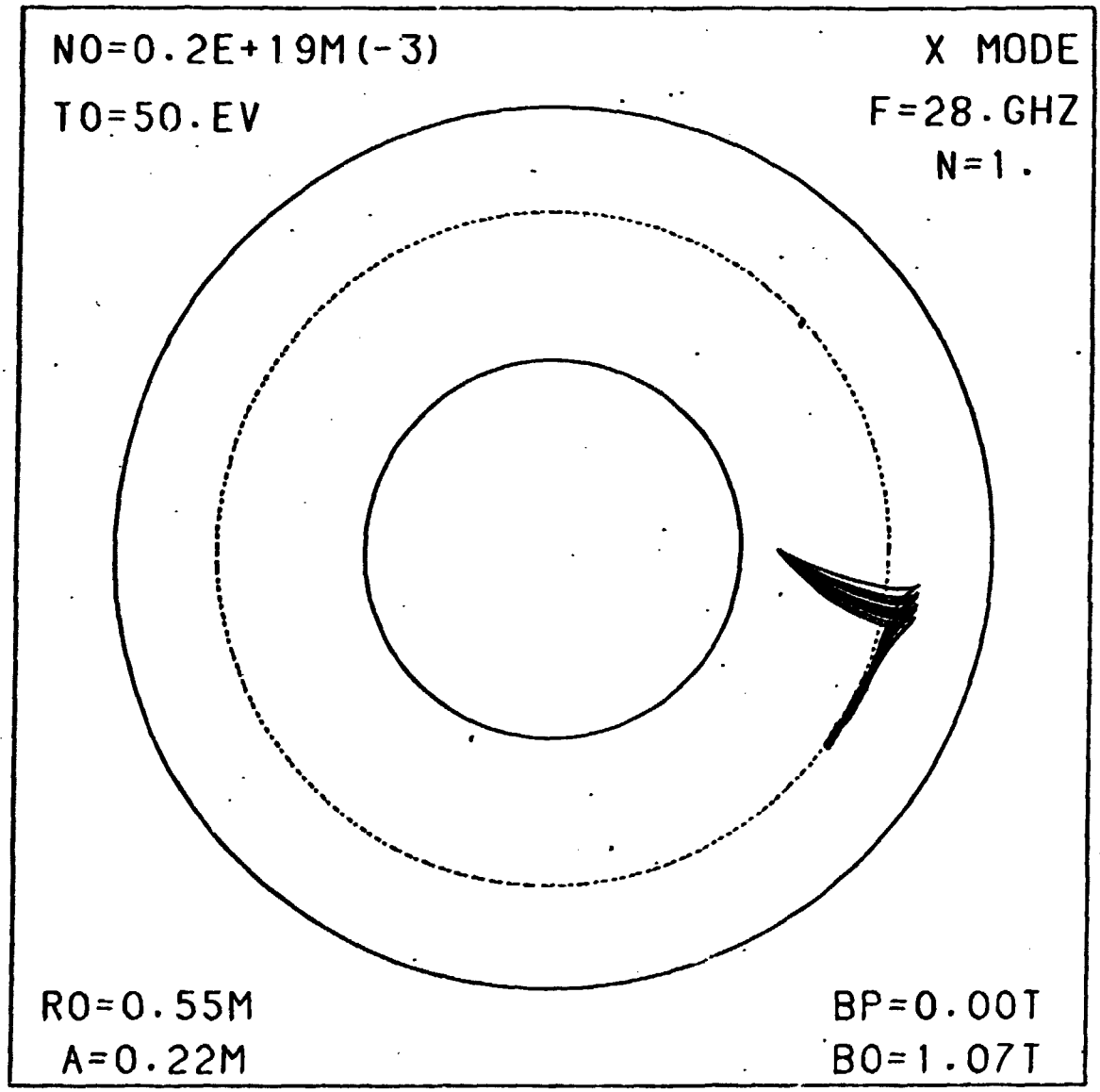

Fig. 2 - A. Montes and G.O. Ludwig

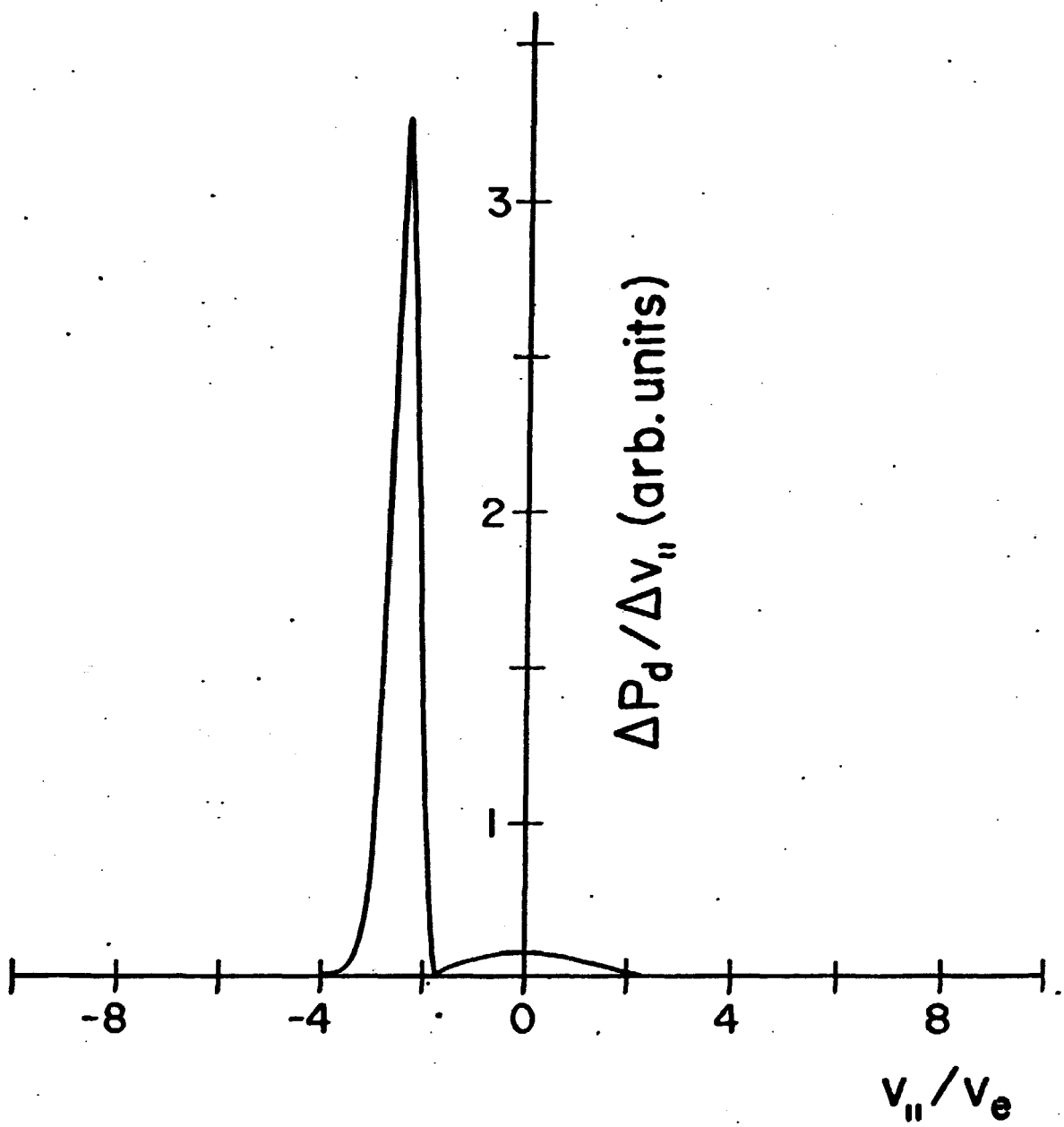

Fig. 3 - A. Montes and G.O. Ludwig

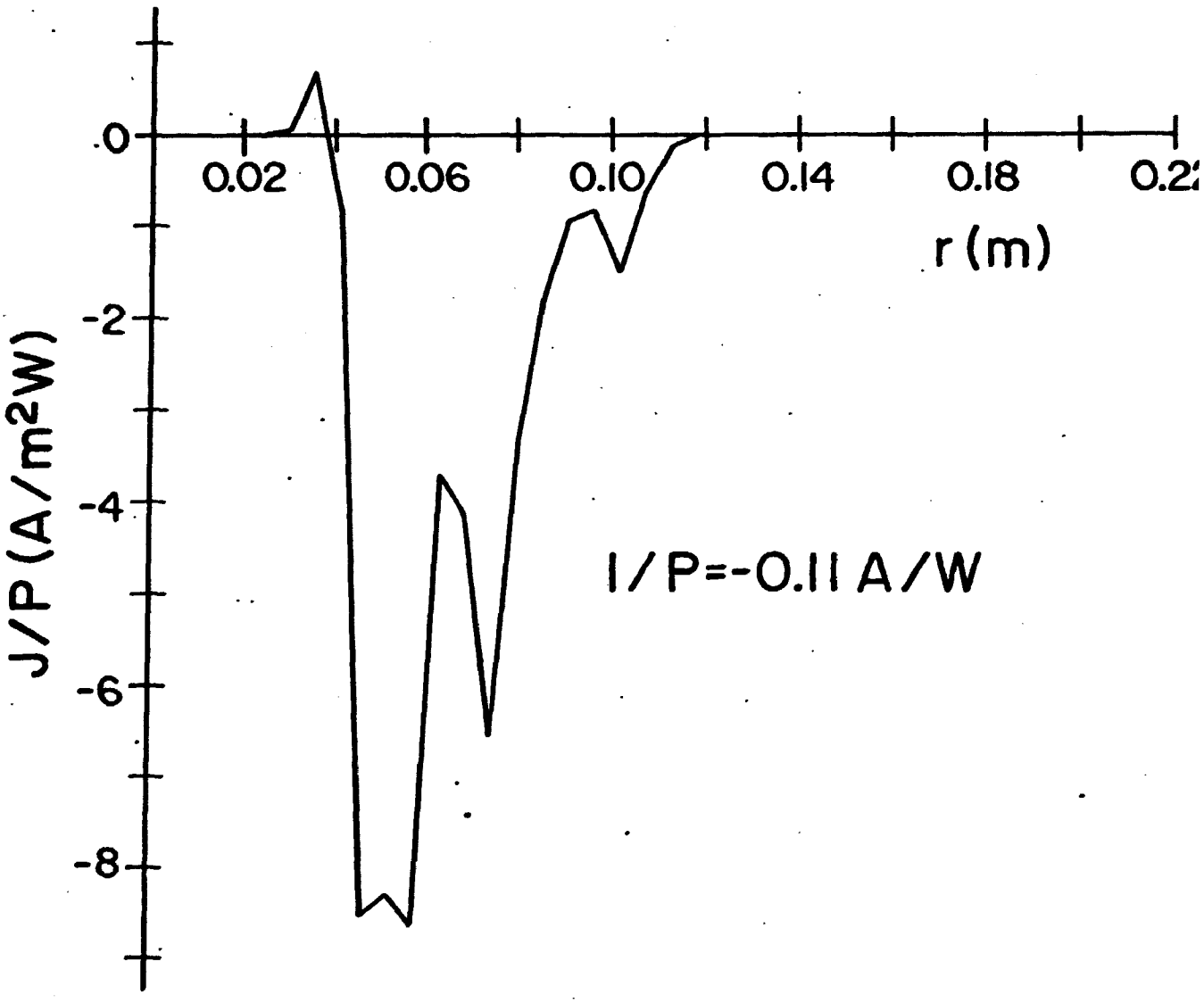

Fig. 4 - A. Montes and G.O. Ludwig

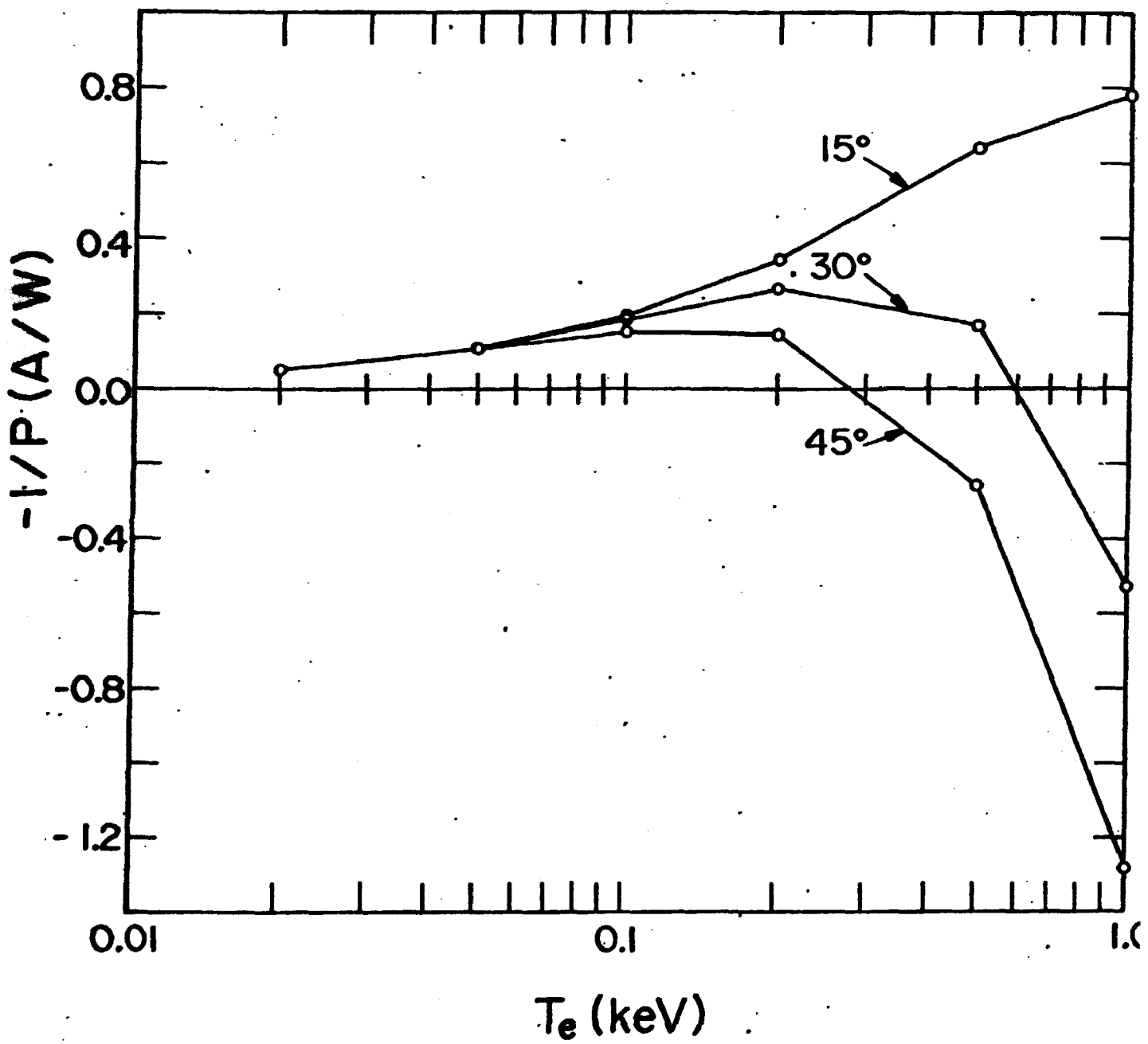

Fig. 5 - A. Montes and G.O. Ludwig